

Serum retinol-binding protein-induced endothelial inflammation is mediated through the activation of toll-like receptor 4

Mei Du,^{1,4} Ashley Martin,^{1,4} Franklin Hays,^{2,4} Jennifer Johnson,² Rafal A. Farjo,³ Krysten M. Farjo^{1,4}

¹Department of Physiology, University of Oklahoma Health Sciences Center, Oklahoma City, OK; ²Department of Biochemistry, University of Oklahoma Health Sciences Center, Oklahoma City, OK; ³EyeCRO LLC, Oklahoma City, OK; ⁴Harold Hamm Diabetes Center, University of Oklahoma Health Sciences Center, Oklahoma City, OK

Purpose: Elevation of serum retinol-binding protein 4 (RBP4) induces inflammation in primary human retinal microvascular endothelial cells (HRECs) via a retinol-independent mechanism; thus, it may play a causative role in the development and progression of vascular lesions in diabetic retinopathy (DR). Since HRECs do not express the classical RBP4 receptor, stimulated by retinoic acid gene 6 (STRA6), this study focuses on identifying the endothelial cell receptor and signaling that mediate RBP4-induced inflammation.

Methods: HRECs were treated with a toll-like receptor 4 (TLR4) small molecule inhibitor (Cli95, also known as TAK-242), TLR4 neutralizing antibody, or mitogen-activated protein kinase (MAPK) inhibitors before treatment with purified recombinant RBP4. The HREC inflammatory response was quantified by in vitro leukostasis assays, western blotting, and enzyme-linked immunosorbent assay (ELISA). To understand how the serum binding partner for RBP4, transthyretin (TTR), may affect RBP4 activity, we also measured RBP4 and TTR levels in serum and retinal lysates from *RBP4-Tg* and wild-type mice.

Results: TLR4 inhibition significantly reduced RBP4-induced expression of pro-inflammatory proteins and in vitro leukostasis. RBP4 treatment significantly increased phosphoactivation of p38 and c-Jun N-terminal protein kinase (JNK). The p38 inhibitor (SB203580) attenuated RBP4-stimulated vascular cell adhesion molecule 1 (VCAM-1), intracellular adhesion molecule 1 (ICAM-1), monocyte chemoattractant protein (MCP-1), and interleukin 6 (IL-6) production, while the JNK inhibitor (SP600125) reduced RBP4-stimulated sICAM-1, endothelial cell selectin (E-selectin), and MCP-1 production. The MAPK inhibitors only showed partial (50–70%) suppression of the RBP4-stimulated proinflammatory response. Moreover, TLR4 inhibition did not decrease RBP4-induced MAPK phosphoactivation, suggesting that RBP4-mediated MAPK activation is TLR4 independent and occurs through a secondary unknown receptor. We also found that the RBP4/TTR molar ratio was exceptionally high in the retina of *RBP4-Tg* mice, indicating an abundance of TTR-free RBP4.

Conclusions: RBP4-induced inflammation is largely mediated by TLR4, and in part, through JNK and p38 MAPK signaling. The high TTR/RBP4 molar ratio in serum likely protects the endothelium from the proinflammatory effects of RBP4 in vivo, whereas elevation of serum RBP4 causes a significant increase in TTR-free RBP4 in retinal tissue. This offers insight into how *RBP4-Tg* mice can develop retinal neurodegeneration without coincident retinal microvascular pathology.

Retinol-binding protein 4 (RBP4) is a novel adipokine (adipose-derived cytokine) that is clinically associated with obesity, insulin resistance, type 2 diabetes (T2DM), and cardiovascular disease [1-11]. In addition, patients with proliferative diabetic retinopathy (DR) have increased serum RBP4 levels compared to diabetic patients with mild or no retinopathy [12,13], which raises the possibility that RBP4 is somehow involved in the pathogenesis of DR. We demonstrated previously that RBP4 elevation induces inflammation in primary human retinal microvascular endothelial cells (HRECs) and human umbilical vein endothelial cells

(HUVECs) by increasing the expression of proinflammatory cytokines, chemokines, and adhesion molecules, including interleukin 6 (IL-6), monocyte chemoattractant protein (MCP-1), endothelial cell selectin (E-selectin), vascular cell adhesion molecule 1 (VCAM-1), and intracellular adhesion molecule 1 (ICAM-1) [14]. We have also shown that RBP4-induced endothelial inflammation is retinol independent and involves activation of nuclear factor κ B (NF- κ B) [14]. In the present study, we used HRECs as a model system to learn more about the cell receptor and signaling pathways that modulate the proinflammatory activity of RBP4.

The upstream mechanisms of RBP4-induced endothelial (HREC) inflammation are unclear. We have shown that the primary RBP4 receptor, stimulated by retinoic acid gene 6 (STRA6), is not expressed in HRECs or HUVECs [14]. Therefore, RBP4 must activate an alternative receptor

Correspondence to: Krysten M. Farjo, University of Oklahoma Health Sciences Center, 940 Stanton L Young Blvd, BMSB 617, Oklahoma City, OK 73104; Phone: (405) 271-8001 ext. 48446; FAX: (405) 271-3181; email: Krysten-farjo@ouhsc.edu

signaling pathway to induce endothelial inflammation. Others have shown that RBP4 impairs insulin signaling in adipocytes indirectly by inducing proinflammatory cytokines in macrophages through retinol-independent, toll-like receptor 4 (TLR4)- and c-Jun N-terminal protein kinase (JNK)-dependent signaling pathways [15]. Moreover, in mice overexpressing RBP4 (Gene ID: 5950, OMIM 180250; *RBP4-Tg*), RBP4 triggers adipose tissue inflammation and insulin resistance via the activation of antigen-presenting cells in adipose tissue through a JNK-dependent pathway that does not involve STRA6 [16]. Thus, the present study investigated whether TLR4 mediates RBP4-induced endothelial inflammation by using a selective TLR4 antagonist small molecule inhibitor (Cli95, also known as TAK-242), TLR4 neutralizing antibody, and specific inhibitors targeting the p38, JNK, and extracellular signal-regulated kinase (ERK) mitogen-activated protein kinases (MAPKs) to evaluate the effect of blocking TLR4 and its downstream signaling on RBP4-induced endothelial inflammation.

METHODS

Purified RBP4: Recombinant human histidine (His)-tagged RBP4 was expressed in *Escherichia coli* and purified as described previously [14], with some modifications to improve protein yield and quality. The cDNA encoding human RBP4 was subcloned into a pBAD-His expression vector (Invitrogen, ThermoFisher Scientific, Waltham, MA) to ensure tight induction control of RBP4 expression. *E. coli* strain BL21-A1 cells, transformed with the pBAD-His-RBP4 expression vector, were induced by addition of 0.2% (w/v) arabinose in working volumes of 2–4 l and grown overnight. His-tagged RBP4 was purified as described previously [14]. Briefly, cells were harvested by centrifugation at 4,000 ×g. Cell pellets were resuspended in lysis buffer (50 mM Tris, pH 7.5, 2 mM EDTA, 1 mM 4-(2-aminoethyl)benzenesulfonyl fluoride hydrochloride (AEBSF), 0.1% Triton X-100). The cell suspension was sonicated 5 times for 20 seconds, freeze-thawed twice and centrifuged at 10,000 ×g for 25 min to pellet the insoluble fraction. The insoluble pellet fraction was solubilized in 5 M guanidine hydrochloride containing 10 mM dithiothreitol with vigorous stirring at room temperature (RT) for 6 h and then batch bound overnight at 4 °C to nickel resin. Following purification of His-RBP4 by nickel affinity chromatography, the protein underwent oxidative refolding, as previously described [14]. For purification of retinol-bound (holo) RBP4 (holo-RBP4), an approximately 10-fold molar excess of retinol was included in the refolding buffer, and all steps after the addition of retinol were performed in a dark room lit by dim red light. After refolding, the protein was

exchanged through dialysis into PBS (1.8 mM KH_2PO_4 , 10 mM Na_2HPO_4 , 137 mM NaCl, 2.7 mM KCl) and purified by size exclusion chromatography (SEC) to select fractions of properly folded His-RBP4, which constituted approximately 80% of the nickel-purified protein. Samples were concentrated before SEC using a 50-ml stirred cell (Amcicon catalog no. 5122, Millipore; Billerica, MA) with an Ultracel 10 kDa Ultrafiltration Disk (Millipore catalog no. 13622, Millipore), to a final volume of approximately 10 ml under 30 psi N_2 . All SEC was performed on a Hitachi Chromaster system using a SuperDex 200 10/300GL column (GE Healthcare catalog no. 17517501, GE Healthcare Life Sciences, Marlborough, MA) and following ultraviolet (UV; 260 nm, 280 nm, and 330 nm) and refractive index signals. Retinol-free (apo) His-tagged RBP4 (His-apo-RBP4) was used for the studies illustrated in Figure 1, Figure 2, and Figure 3 to ensure that all RBP4 activity was retinoid independent, although similar results were obtained with retinol-bound His-holo-RBP4 protein. As in our previous study, we tested the level of endotoxin contamination in purified RBP4 protein and found that it was below the level of endotoxin present in the PBS solvent used for dissolving RBP4 and negative control protein bovine serum albumin (BSA).

HREC culture: Primary HRECs were obtained from the Cell Systems Corporation (Kirkland, WA) and cultured in EGM-MV (Promocell, Germany) at 37 °C in 5% CO_2 and 95% air. The cells were grown and maintained on collagen I-coated tissue culture plates from Corning Life Sciences (Kennebunk, ME). For the experiments, HREC confluent monolayers were incubated in endothelial cell basal media with 2% (v/v) fetal bovine serum (FBS) for 8–16 h to induce quiescence. All experiments were conducted using HRECs at passages 4 to 11, as we confirmed that cells maintained similar viability up to passage 11 (data not shown). TLR4 receptor inhibitor and MAPK inhibitor studies were conducted by preincubating cells with the inhibitors for 2 h before the addition of RBP4 at 100 $\mu\text{g}/\text{ml}$. TLR4 chemical inhibitor Cli95 (aka TAK-242), TLR4 neutralizing antibody TLR4 neutralizing monoclonal antibody (mAb), and control immunoglobulin G (IgG) were purchased from InvivoGen (San Diego, CA). The MAPK inhibitors SP600125, SB203580, and U0126 were purchased from Cell Signaling Technology Inc. (Danvers, MA).

Culture of THP-1 cells and in vitro leukostasis assay: The human monocytic cell line (THP-1) was obtained from the American Type Culture Collection (Manassas, VA) and cultured in Roswell Park Memorial Institute (RPMI) 1640 medium containing 10% (v/v) FBS and 0.05 mM β -mercaptoethanol. Leukocyte adhesion assay was performed

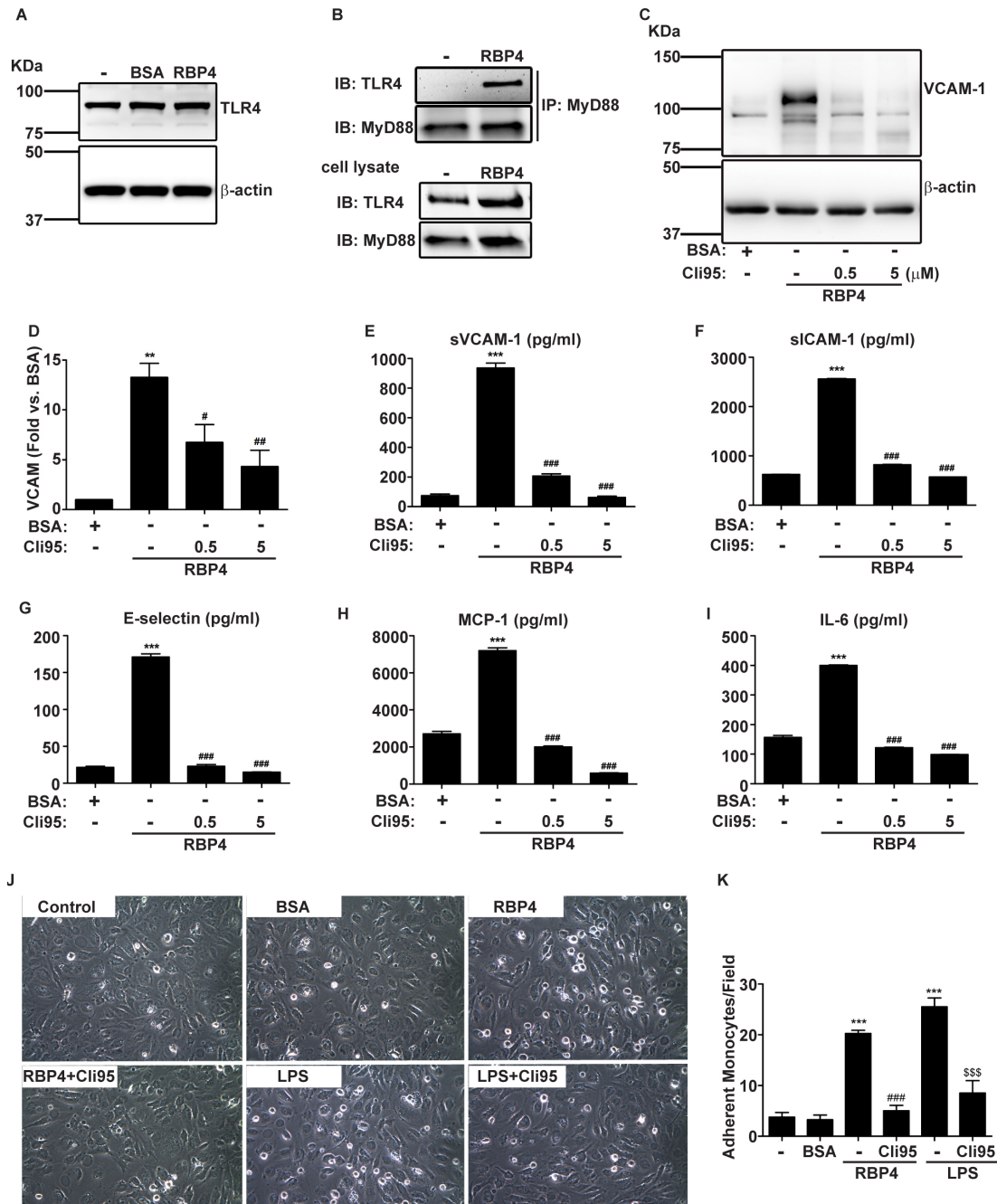


Figure 1. Chemical inhibition of toll-like receptor 4 (TLR4) blocks retinol-binding protein 4 (RBP4)-induced endothelial inflammation. **A:** TLR4 expression in human retinal microvascular endothelial cells (HRECs) with and without treatment with 100 μ g/ml RBP4 or the molar equivalent of bovine serum albumin (BSA) for 24 h. **B:** Interaction between TLR4 and adaptor molecule MyD88 in HRECs with and without RBP4 treatment for 30 min was analyzed with immunoprecipitation (IP) and immunoblotting. Expression of TLR4 and MyD88 was analyzed by immunoblotting using total cell lysates. **C** and **D:** Western blot and densitometry analyses of vascular cell adhesion molecule 1 (VCAM-1) protein expression in HRECs treated with RBP4 in the absence or presence of a 2-h preincubation of TLR4 chemical inhibitor Cli95. Bar graph data represent the mean \pm standard deviation (SD) of three independent experiments. **E-I:** Enzyme-linked immunosorbent assay (ELISA)-based quantification of soluble extracellular levels of (E) VCAM-1, (F) intracellular adhesion molecule 1 (ICAM-1), (G) endothelial cell selectin (E-selectin), (H) monocyte chemoattractant protein (MCP-1), and (I) interleukin 6 (IL-6) in HREC media. **J:** Representative phase-contrast images of leukocyte adhesion to HRECs after the indicated treatment. Data are representative of four separate experiments. Magnification: 20 \times . **K:** The number of leukocytes adhering to HRECs was counted in four randomly selected visual fields (20 \times objective) for each treatment group. **, $p < 0.01$; ***, $p < 0.001$ versus BSA; #, $p < 0.05$; ##, $p < 0.01$; ###, $p < 0.001$ versus RBP4; \$\$\$, $p < 0.001$ versus lipopolysaccharide (LPS) by one-way analysis of variance (ANOVA) with Tukey's post hoc test.

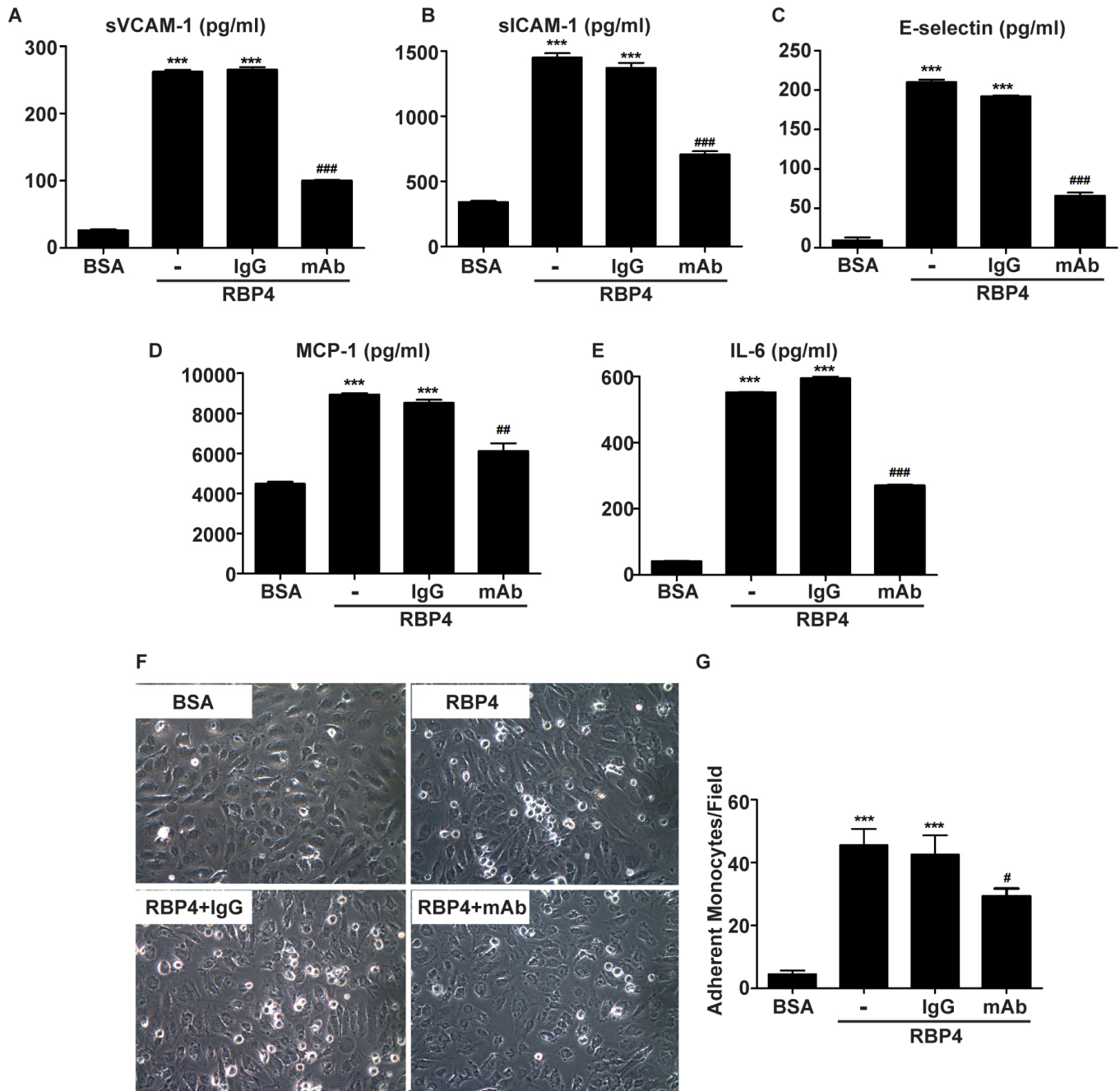


Figure 2. Neutralizing antibody against toll-like receptor 4 (TLR4) reduces retinol-binding protein 4 (RBP4)-induced endothelial inflammation. **A-E**: Human retinal microvascular endothelial cells (HRECs) were exposed to TLR4 neutralizing antibody (mAb) or control immunoglobulin G (IgG) at 10 μ g/ml for 2 h, followed by RBP4 treatment for 24 h. Cell media were collected for enzyme-linked immunosorbent assay (ELISA)-based quantification of soluble extracellular levels of (A) vascular cell adhesion molecule 1 (VCAM-1), (B) intracellular adhesion molecule 1 (ICAM-1), (C) endothelial cell selectin (E-selectin), (D) monocyte chemoattractant protein (MCP-1), and (E) interleukin 6 (IL-6). **F**: Representative images of monocyte adherence to HRECs after the indicated treatment. Data are representative of three separate experiments. Magnification: 20 \times . **G**: Adherent monocytes were counted in four randomly selected visual fields (20 \times objective) for each treatment group. ***, $p < 0.001$ versus bovine serum albumin (BSA); #, $p < 0.05$; ##, $p < 0.01$; ###, $p < 0.001$ versus RBP4 by one-way analysis of variance (ANOVA) with Tukey's post hoc test.

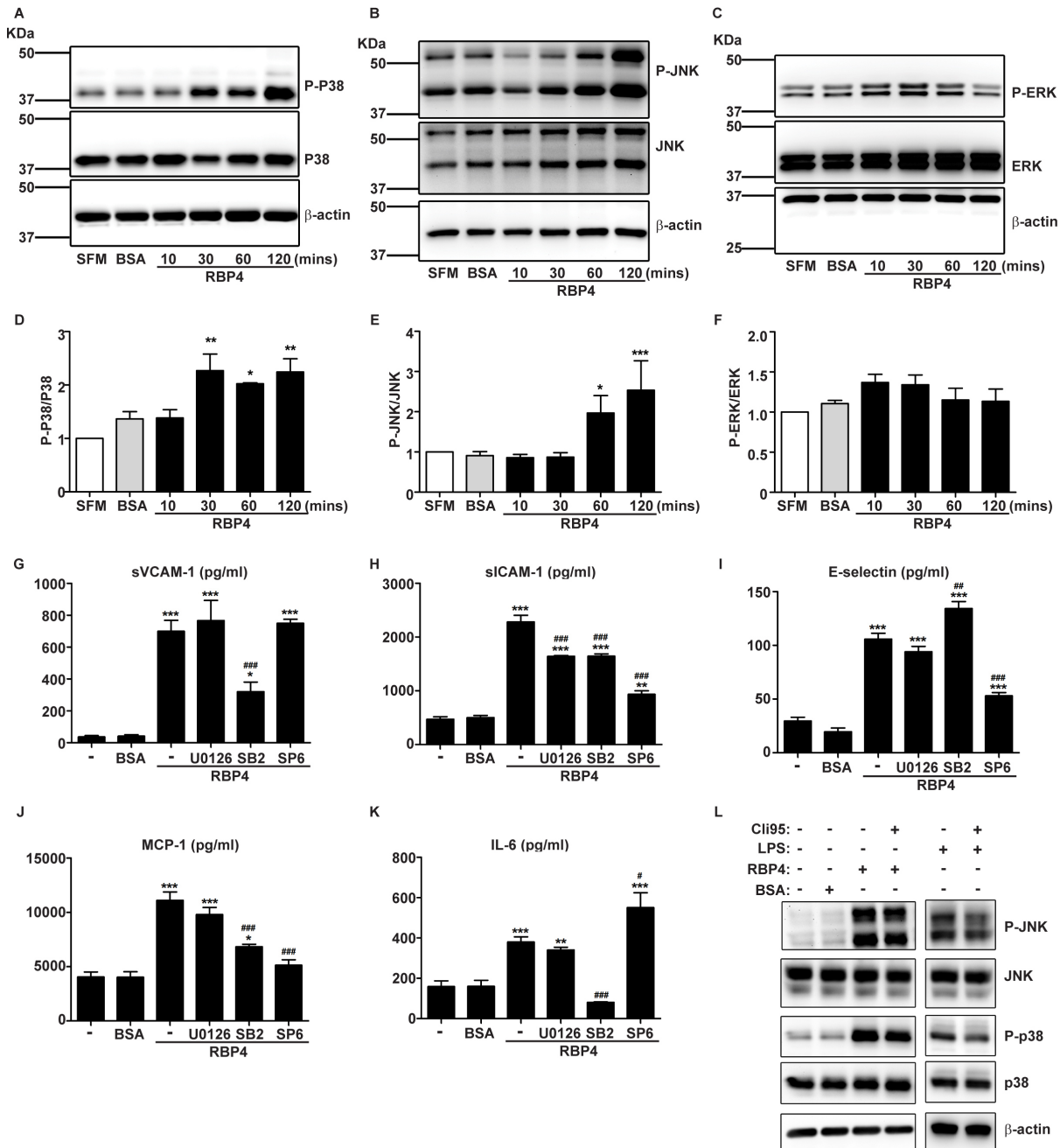


Figure 3

Figure 3. Activation of p38 and c-Jun N-terminal protein kinase (JNK) at least partially mediates the effects of retinol-binding protein 4 (RBP4) on cytokine production in human retinal microvascular endothelial cells (HRECs). **A-C:** RBP4 triggers phosphoactivation of **(A)** p38, **(B)** JNK, and **(C)** extracellular signal-regulated kinase (ERK) in HRECs for the indicated times from 10 min to 2 h. SFM: serum-free media only. **D-F:** Quantification of experiments shown in panel **A-C**. Phosphorylated proteins in each immunoblot are normalized to total protein content of the respective protein. Values are means \pm standard error of the mean (SEM), $n=3$. *, $p<0.05$; **, $p<0.01$; ***, $p<0.001$, versus SFM by one-way analysis of variance (ANOVA) with Tukey's post hoc test. **G-K:** HRECs were pretreated with U0126 (ERK1/2 inhibitor, 10 μ M), SB203580 (p38 inhibitor, 10 μ M), and SP600125 (JNK inhibitor, 50 μ M) for 2 h before incubating with RBP4 for 24 h; culture media were then collected for enzyme-linked immunosorbent assay (ELISA) -based quantification of soluble extracellular levels of **(G)** vascular cell adhesion molecule 1 (VCAM-1), **(H)** intracellular adhesion molecule 1 (ICAM-1), **(I)** endothelial cell selectin (E-selectin), **(J)** monocyte chemoattractant protein (MCP-1), and **(K)** interleukin 6 (IL-6). *, $p<0.05$; **, $p<0.01$; ***, $p<0.001$, versus bovine serum albumin (BSA); #, $p<0.05$; ##, $p<0.01$; ###, $p<0.001$ versus RBP4 by one-way ANOVA with Tukey's post hoc test. **L:** HRECs were pretreated with ClI95 (0.5 μ M) for 2 h before addition of RBP4 or LPS as a positive control for 24 h. Cell lysates were analyzed by western blotting as indicated.

as previously described [14]. Briefly, HRECs were grown to confluence in six-well plates and treated in serum-starved 2% (v/v) FBS medium with BSA or RBP4 for 20 h with or without a 2 h preincubation with TLR4 inhibitors. THP-1 monocytes were seeded at 1.25 million cells/well and co-cultured with HRECs for 3 h. Unbound THP-1 monocytes were thoroughly removed by gently washing 3X with PBS, and cells were fixed in 4% (v/v) paraformaldehyde for 10 min. Adherent monocytes were photographed using phase-contrast microscopy at a magnification of 20 \times , and they were counted/scored in at least four random fields for each treatment.

ELISAs: HREC culture media were collected after the indicated treatments, centrifuged at 10,000 \times g for 2 min to remove cell debris, and stored at -80°C . Expression of proinflammatory molecules in cell culture supernatant was determined by sandwich enzyme-linked immunosorbent assay (ELISA) according to the manufacturer's instructions. ELISA kits from R&D Systems, Inc. (Minneapolis, MN) were used to measure soluble extracellular levels of VCAM-1 (catalog no. DY809), ICAM-1 (catalog no. DY720), MCP-1 (catalog no. DY279), IL-6 (catalog no. DY206), and E-selectin (catalog no. DY724).

Immunoprecipitation and western blot analysis: Cell extracts were prepared by homogenization in lysis buffer containing 50 mM Tris, pH 7.4, 40 mM NaCl, 1 mM EDTA, 50 mM NaF, 10 mM $\text{Na}_4\text{P}_2\text{O}_7$, 10 mM sodium β -glycerol phosphate, 0.5% (v/v) Triton X-100, and 100 \times phosphatase and protease inhibitor cocktail, as described previously [17]. Cell debris was removed by centrifugation, the supernatant was collected, and protein concentration was determined by Bradford assay. A total of 1 mg of protein was incubated with the MyD88 antibody (catalog no. 4283, Cell Signaling Technology; Danvers, MA). Immunoprecipitates were washed 5X with lysis buffer, boiled in Laemmli buffer (100 mM Tris, pH 6.8 RT, 200 mM dithiothreitol, 4% (w/v) sodium dodecyl sulfate [SDS], 0.2% (w/v) bromophenol blue, 1 mM 4-(2-aminoethyl) benzenesulfonyl fluoride hydrochloride (AEBSF), 20% (v/v) glycerol) for 5 min, and analyzed by western blotting.

For western blot analysis, cells or tissues were lysed in Laemmli buffer, resolved by SDS-polyacrylamide gel electrophoresis (PAGE), and subjected to immunoblotting analysis with the indicated antibodies. The following antibodies were used: from Santa Cruz Biotechnology (Dallas, TX), TLR4 (catalog no. sc-293072), β -actin (catalog no. sc-47778), and VCAM-1 (catalog no. SC-8304); from Cell Signaling Technology, JNK (catalog no. 9258), (P) JNK (phospho-Thr183/Tyr185; catalog no. 4668), p38 (catalog no. 8690), (P) p38 (phospho-Thr180/Tyr182; catalog no. 4511), ERK, (catalog no. 4695), and (P) ERK (phospho-Thr202/

Tyr204; catalog no. 4370); and from Novus Biologicals (Littleton, CO), GAPDH (catalog no. NB300-221). Band intensities were normalized to β -actin or GAPDH and quantified using UVP analyzing software (BioSpectrum® Imaging System, UVP, Upland, CA).

Mice: *RBP4-Tg* mice, which overexpress human RBP4 under control of the mouse muscle creatine kinase (MCK) promoter on a C57BL/6J background, have been described previously [18], and the animals were kindly provided by Loredana Quadro. All animal studies were approved by the Institutional Animal Care and Use Committee of the University of Oklahoma Health Sciences Center (OUHSC) and adhered to the Association for Research in Vision and Ophthalmology (ARVO) Statement for the Use of Animals in Ophthalmic and Vision Research. Mice were fed a standard chow diet (Labdiet 5001) ad libitum. This diet contained a sufficient amount of vitamin A (15 IU g^{-1}). All studies were performed on age-, sex-, and strain-matched wild-type controls. Both sexes were used in all studies, and no sex-dependent differences in phenotype were observed.

Mouse serum was collected by superficial temporal vein puncture from live mice that had fasted for 6 h. Retinal tissue was dissected after mice were euthanized by CO_2 asphyxiation and quickly perfused with PBS at a flow rate of 8 ml/min for 3 min to remove blood cells. Retinas were rapidly collected using Winkler's method, snap frozen, and stored at -80°C . The retinas were suspended in lysis buffer (50 mM Tris-HCl, pH 7.8, 0.1 M NaCl, 5 mM EDTA, 0.1% [w/v] SDS, 1 mM 4-(2-aminoethyl) benzenesulfonyl fluoride hydrochloride, 0.1% (w/v) Triton X-100, 2.5% [v/v] glycerol) and sonicated on ice at a 20% intensity for two rounds of 5 s each. Insoluble material was removed by centrifugation, and the protein concentration was determined by Bradford colorimetric assay. ELISA kits for mouse TTR (catalog no. IRKTAH1161; Innovative Research, Novi, MI), mouse RBP4 (catalog no. MRB400; R&D Systems, Minneapolis, MN), and human RBP4 (catalog no. DRB400; R&D Systems) were used to quantify target molecules in serum and retina lysates. RBP4 and TTR levels in retina lysates were normalized according to the total retinal protein content in each sample.

Statistical analysis: Data are presented as mean \pm standard deviation (SD). Statistical analyses were conducted using Prism 4 software (La Jolla, CA) with one-way analysis of variance (ANOVA) using Tukey's post hoc analysis to compare differences among three or more groups. A value of $p < 0.05$ was accepted as significant.

RESULTS

RBP4-induced endothelial inflammation is TLR4-dependent:

We first examined TLR4 protein expression in HRECs by western blot. We observed abundant expression of TLR4 in HRECs, and RBP4 treatment did not change the expression level of TLR4 protein (Figure 1A). Next, we sought to determine whether RBP4 activates TLR4 signaling in HRECs. TLR4 is known to signal via binding interaction with an adaptor protein, MyD88 [19,20]. Therefore, we performed coimmunoprecipitation (co-IP) to assess whether RBP4 treatment promotes MyD88 binding to TLR4. We observed increased interaction between TLR4 and MyD88 in HREC lysate at 30 min after RBP4 treatment (Figure 1B), suggesting that RBP4 activates MyD88-dependent TLR4 signaling in HRECs. To further address whether TLR4 is the membrane receptor that mediates RBP4-induced inflammation in HRECs, we applied a specific chemical inhibitor of TLR4, Cli95, which is a small molecule that binds to the intracellular domain of TLR4 at cysteine-747 and inhibits TLR4 adaptor protein-protein interaction and signaling [21,22]. Cli95 significantly decreased RBP4-mediated induction of cellular VCAM-1 protein (Figure 1C,D) and reduced extracellular soluble protein levels of VCAM-1, ICAM-1, E-selectin, MCP-1, and IL-6 (Figure 1E-I). Similarly, pretreatment with TLR4 neutralizing antibody, but not control IgG, significantly blocked RBP4-mediated induction of proinflammatory factors (Figure 2A-E).

We previously showed by *in vitro* leukostasis assays that RBP4-induced expression of proinflammatory genes leads to increased monocyte adherence on HREC monolayers [14]. Herein, we performed *in vitro* leukostasis assays to quantify the net effect of TLR4 inhibition on RBP4-induced inflammation. Consistent with our previous findings, HRECs treated with RBP4 (100 µg/ml), or lipopolysaccharide (LPS) as a positive control, showed significantly increased leukostasis compared to negative controls (Figure 1J,K; $p < 0.001$; $n = 4$). RBP4-induced leukostasis was significantly inhibited in HRECs pretreated with TLR4 chemical inhibitor (Figure 1J,K) or TLR4 neutralizing antibody (Figure 2F,G), demonstrating that RBP4-induced HREC inflammation is largely TLR4-dependent.

RBP4 induces proinflammatory molecules through the activation of JNK and P38 signaling: Previous studies have shown that stimulation of TLR4 can initiate phosphorylation of three MAPKs, namely JNK, p38, and ERK, which leads to subsequent cytokine secretion [23]. Other studies have revealed that RBP4 causes insulin resistance in adipocytes by inducing proinflammatory cytokines in macrophages through a JNK- and TLR4-dependent mechanism [15]. To

determine whether RBP4 activates the MAPK signaling pathway to promote inflammation in HRECs, we measured the phosphoactivation of MAPKs by western blot. Within 30–120 min of RBP4 treatment, HRECs exhibited significantly increased phosphoactivation of p38 (Figure 3A,D) and JNK (Figure 3B,E). Phosphorylated ERK1/2 showed a trend toward increased expression at 10–30 min, but this did not reach statistical significance (Figure 3C,F).

To further investigate the role of MAPK signaling pathways in RBP4-mediated cytokine production, we employed specific inhibitors of p38, JNK, and ERK. The p38 inhibitor (SB203580) attenuated RBP4-stimulated sVCAM-1, sICAM-1, MCP-1, and IL-6 production, while the JNK inhibitor (SP600125) reduced RBP4-stimulated sICAM-1, E-selectin, and MCP-1 production (Figure 3G-K). The ERK inhibitor (U0126) only showed inhibitory effect on sICAM-1 production (Figure 3H). The MAPK inhibitors only showed partial (50–70%) suppression of the RBP4-stimulated proinflammatory response (Figure 3G-K). Moreover, TLR4 inhibition does not decrease RBP4-induced MAPK phosphoactivation (Figure 3L), suggesting that RBP4-mediated MAPK activation is TLR4 independent and occurs through a secondary unknown receptor. Taken together, these results suggest that RBP4-induced endothelial inflammation is mediated in part through the activation of the JNK and p38 pathways.

The RBP4 level exceeds the binding capacity of transthyretin in neuronal retinal tissue: Our previous study found no retinal microvascular pathology in *RBP4-Tg* mice aged up to 6 months [24], which is perplexing, as the data herein and in our previous study [14] clearly showed that RBP4 can induce endothelial inflammation in cultured HRECs. In plasma, RBP4 (95%) is mostly found in a complex with its carrier transthyretin (TTR), which increases its molecular mass, thereby preventing its removal by glomerular filtration [25]. Previous studies reported that association with TTR can stabilize RBP4 and block receptor binding and subsequent activation of cell signaling [26,27]. TTR is normally present in three- to fivefold molar excess to RBP4 in human [26,28] and rodent serum [24]. We speculated that the high molar ratio of TTR/RBP4 in serum, which is maintained even in *RBP4-Tg* mice (Figure 4B), facilitates TTR-mediated inhibition of RBP4 pro-inflammatory activity to protect endothelium, including the retinal microvasculature, *in vivo*.

Intriguingly, our previous study found that *RBP4-Tg* mice have early-onset progressive retinal neurodegeneration [24]. We have previously shown that *RBP4-Tg* mice have a ~7-fold increase in retinal RBP4 level relative to wild-type mice [24]. Thus, to address whether TTR-mediated inhibition of RBP4 proinflammatory activity is possible in the neuronal retina,

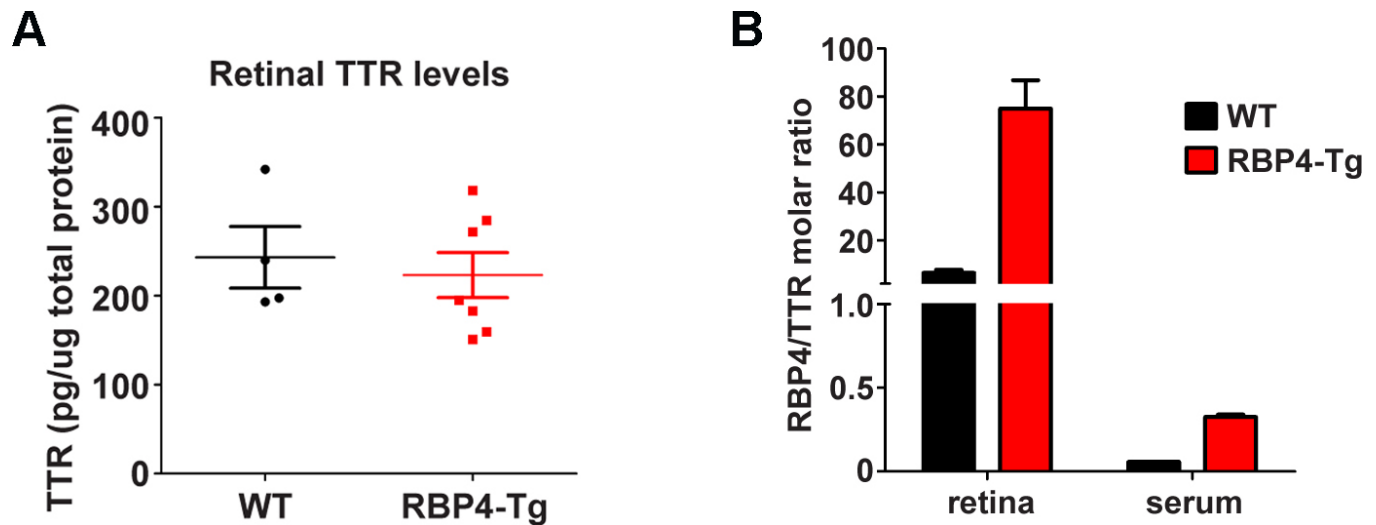


Figure 4. The retinol-binding protein 4 (RBP4)/transthyretin (TTR) molar ratio is extremely high in neuronal retina tissue. **A:** TTR levels in perfused retinal neuronal tissue lysates from wild-type and *RBP4-Tg* mice were measured by enzyme-linked immunosorbent assay (ELISA). **B:** RBP4/TTR molar ratio in mouse serum versus retina. *RBP4-Tg* and WT mice aged 10 weeks (serum samples) and 6 months (retinal lysate) was used to measure RBP4 and TTR levels by ELISA. Values are mean \pm standard deviation (SD); $n \geq 5$ mice per genotype. Student's t-test confirms that the means in panel B have a statistical difference between wild-type and *RBP4-Tg* of $p < 0.01$ for the retina, and $p < 0.001$ for serum.

we measured the level of TTR present in perfused retinal neuronal tissue lysates from wild-type and *RBP4-Tg* mice. The TTR levels in *RBP4-Tg* retinas were similar to those in wild-type mice (Figure 4A), meaning that retinal tissue has an extremely high RBP4/TTR molar ratio (about 70) in *RBP4-Tg* mice (Figure 4B). This suggests that the increased levels of RBP4 present in the retina of *RBP4-Tg* mice may promote retinal neurodegeneration due to the lack of TTR-mediated inhibition of RBP4.

DISCUSSION

Recent studies revealed that RBP4 is a proinflammatory adipokine associated with obesity [1,2], insulin resistance [1-6], cardiovascular disease [7-11], and T2DM and its microvascular complications [2,6,13,29]. While a proinflammatory effect of RBP4 has been implicated in these diseases, the underlying cellular mechanisms are not understood. TLR4 and other receptors involved in the innate immune response recognize damage-associated molecule patterns (DAMPs) from endogenous proteins that are elevated due to stress, inflammation, and cell death. Recent studies have shown that the retinol-independent proinflammatory activity of RBP4 in adipose tissue is mediated through TLR4 activation [15,16]. The data herein showed that TLR4 inhibition significantly blocked RBP4-induced expression of proinflammatory genes, including VCAM-1, ICAM-1, IL-6, MCP-1, and E-selectin, in HRECs. We also observed phosphoactivation of MAPK

signaling in response to RBP4 treatment, and MAPK inhibitors significantly reduced RBP4-mediated expression of proinflammatory genes. Thus, this is the first study to show that RBP4-induced inflammation in HRECs is largely mediated by TLR4, and in part, through JNK and p38 MAPK signaling.

RBP4 induces phosphoactivation of p38 and JNK, and inhibitors of p38 and JNK activation can partially inhibit RBP4-induced inflammation in HRECs. However, p38 and JNK inhibitors were not as effective in reducing RBP4-induced production of proinflammatory molecules as TLR4 inhibitors were. Moreover, inhibition of TLR4 did not block RBP4-mediated phosphoactivation of p38 and JNK (Figure 3L). These data indicate that p38 and JNK phosphoactivation is mediated through an alternative receptor to TLR4, and that this signaling pathway acts secondarily to the TLR4-dependent pathway to promote inflammation in HRECs. The receptor for advanced glycation end-products (RAGE) is a likely candidate for this alternative RBP4 receptor in HRECs. RAGE is expressed in endothelial cells [30] and activates p38 and JNK signaling to induce inflammation [31-33]. Moreover, RAGE is known to interact and crosstalk with TLR4 (reviewed in [34]). Therefore, it may be that maximal RBP4 proinflammatory action is mediated by cooperative binding and activation of the RAGE/TLR4 complex. Indeed, this could explain why the chemical TLR4 inhibitor Cli95 was more effective at blocking RBP4-induced inflammation

(Figure 1C-K) compared to the TLR4 neutralizing antibody (Figure 2), since Cli95 blocks cellular signaling activation [21,22], whereas the antibody can only block ligand-mediated activation of TLR4, but ligand activation of a TLR4/RAGE complex through binding to RAGE may still be intact.

A substantial body of research has shown that TLR4 is expressed in a variety of ocular tissues and plays an important role in protection against microbial infection [35-38]. In the retina, TLR4 is primarily expressed in microglial cells, but it can also be detected in photoreceptors and Müller cells [39-41]. TLR4 activation promotes retinal degeneration by increasing neuroinflammation, oxidative stress, and mitochondrial DNA damage [42-44]. Moreover, TLR4 deficiency can reduce retinal degeneration [45]. We have previously shown that *RBP4-Tg* mice have early-onset progressive retinal degeneration that features neuroinflammation [24]. Thus, RBP4 may be activating TLR4 in the retina to promote neurodegeneration. Most retinal cells also express RAGE, and RAGE is involved in the pathogenesis of DR, including retinal neurodegeneration [46-48]. Thus, future studies in *RBP4-Tg* mice should investigate whether TLR4 or RAGE contributes to RBP4-induced retinal neurodegeneration.

Interestingly, our previous study found no retinal vascular pathology in *RBP4-Tg* mice aged up to 6 months, despite significant retinal neurodegeneration [24]. Under normal physiological conditions, most RBP4 (95%) circulates in plasma in a complex with TTR at a 1:1 molar ratio, and only a small fraction can be found in serum as TTR-free RBP4 [26]. In addition, serum TTR levels exceed RBP4 levels, even in *RBP4-Tg* mice (Figure 4B). Thus, the high TTR/RBP4 molar ratio in serum likely inhibits RBP4 proinflammatory activity in the retinal vasculature. However, we showed that increased serum RBP4 levels in *RBP4-Tg* mice result in an increased level of TTR-free RBP4 in the neuronal retina (Figure 4B). Therefore, TTR-mediated inhibition of RBP4 activity is largely restricted to the vascular compartment, whereas in peripheral tissues, such as the retina, TTR-free RBP4 is likely more active. This may explain why *RBP4-Tg* mice have early-onset retinal neurodegeneration but no detectable retinal microvascular abnormalities up to 6 months of age.

It is well documented that retinal neurodegeneration precedes retinal microvascular disease in DR [49-74]; therefore, future studies in aged *RBP4-Tg* mice should determine whether retinal microvascular pathology occurs subsequent to retinal neurodegeneration during aging, since RBP4-mediated retinal neurodegeneration could act as an initial trigger to promote both neuronal and vascular damage in DR. Moreover, since elevated RBP4 levels have been clinically

linked to proliferative DR [12,13], as well as cardiovascular disease [7-9,75], it may be that additional factors, such as hyperglycemia, dyslipidemia, or systemic inflammation, can enhance RBP4 proinflammatory action on the endothelium. Notably, *RBP4-Tg* mice have normal bodyweight, blood glucose, and triglyceride levels [24]. Thus, *RBP4-Tg* mice may develop more severe retinal microvascular disease than wild-type mice in response to a high-fat diet or genetically or experimentally induced diabetes, although this requires further investigation. Surprisingly, we found that neither *db/db* nor streptozotocin (STZ)-induced diabetic mice develop elevated serum RBP4 levels by 6 months of age (unpublished data, not shown). This finding reveals that elevation of RBP4 is not essential for the development of DR, since both *db/db* and STZ mice develop characteristics of DR before 6 months of age in the absence of RBP4 elevation [76-86]. However, it is unclear how an elevated serum RBP4 level, which is present in a large portion of diabetic patients based on clinical studies [1-6], may affect the progression of DR. Thus, further studies should utilize *db/db* and STZ mice in conjunction with *RBP4-Tg* mice to investigate how elevated serum RBP4 affects the progression and severity of DR.

ACKNOWLEDGMENTS

We thank Loredana Quadro for providing *RBP4-Tg* mice. The research reported in this study was supported by an institutional development award (IDeA) from the National Institute of General Medical Sciences of the National Institutes of Health under grant number P20GM104934 (K.M.F. received funding as a promising junior investigator on this grant), an American Heart Association beginning grant-in-aid (13BGIA16920097; principal investigator, K.M.F.), and a bridge grant from the Presbyterian Health Foundation (K.M.F.).

REFERENCES

1. Aeberli I, Biebinger R, Lehmann R, L'Allemand D, Spinaz GA, Zimmermann MB. Serum retinol-binding protein 4 concentration and its ratio to serum retinol are associated with obesity and metabolic syndrome components in children. *J Clin Endocrinol Metab* 2007; 92:4359-65. [PMID: 17726085].
2. Graham TE, Yang Q, Bluher M, Hammarstedt A, Ciaraldi TP, Henry RR, Wason CJ, Oberbach A, Jansson PA, Smith U, Kahn BB. Retinol-binding protein 4 and insulin resistance in lean, obese, and diabetic subjects. *N Engl J Med* 2006; 354:2552-63. [PMID: 16775236].
3. Bremer AA, Devaraj S, Afify A, Jialal I. Adipose tissue dysregulation in patients with metabolic syndrome. *J Clin Endocrinol Metab* 2011; 96:E1782-8. [PMID: 21865369].

4. Kowalska I, Straczkowski M, Adamska A, Nikolajuk A, Karczewska-Kupczewska M, Oziomek E, Gorska M. Serum retinol binding protein 4 is related to insulin resistance and nonoxidative glucose metabolism in lean and obese women with normal glucose tolerance. *J Clin Endocrinol Metab* 2008; 93:2786-9. [PMID: 18430770].
5. Mostafaie N, Sebesta C, Zehetmayer S, Jungwirth S, Huber KR, Hinterberger M, Leitha T, Hofman J, Hejtman M, Schratlbauer K, Krugluger W, Tragl KH, Fischer P. Circulating retinol-binding protein 4 and metabolic syndrome in the elderly. *Wien Med Wochenschr* 2011; 161:505-10. [PMID: 21442217].
6. Yang Q, Graham TE, Mody N, Preitner F, Peroni OD, Zabolotny JM, Kotani K, Quadro L, Kahn BB. Serum retinol binding protein 4 contributes to insulin resistance in obesity and type 2 diabetes. *Nature* 2005; 436:356-62. [PMID: 16034410].
7. Bobbert T, Raila J, Schwarz F, Mai K, Henze A, Pfeiffer AF, Schweigert FJ, Spranger J. Relation between retinol, retinol-binding protein 4, transthyretin and carotid intima media thickness. *Atherosclerosis* 2010; 213:549-51. [PMID: 20832065].
8. Ingelsson E, Sundstrom J, Melhus H, Michaelsson K, Berne C, Vasani RS, Riserus U, Blomhoff R, Lind L, Arnlov J. Circulating retinol-binding protein 4, cardiovascular risk factors and prevalent cardiovascular disease in elderly. *Atherosclerosis* 2009; 206:239-44. [PMID: 19339013].
9. Sasaki M, Otani T, Kawakami M, Ishikawa SE. Elevation of plasma retinol-binding protein 4 and reduction of plasma adiponectin in subjects with cerebral infarction. *Metabolism* 2010; 59:527-32. [PMID: 19846170].
10. Solini A, Santini E, Madec S, Rossi C, Muscelli E. Retinol-binding protein-4 in women with untreated essential hypertension. *Am J Hypertens* 2009; 22:1001-6. [PMID: 19556974].
11. Bobbert P, Weithauser A, Andres J, Bobbert T, Kuhl U, Schultheiss HP, Rauch U, Skurk C. Increased plasma retinol binding protein 4 levels in patients with inflammatory cardiomyopathy. *Eur J Heart Fail* 2009; 11:1163-8. [PMID: 19926600].
12. Li ZZ, Lu XZ, Liu JB, Chen L. Serum retinol-binding protein 4 levels in patients with diabetic retinopathy. *J Int Med Res* 2010; 38:95-9. [PMID: 20233518].
13. Takebayashi K, Suetsugu M, Wakabayashi S, Aso Y, Inukai T. Retinol binding protein-4 levels and clinical features of type 2 diabetes patients. *J Clin Endocrinol Metab* 2007; 92:2712-9. [PMID: 17440021].
14. Farjo KM, Farjo RA, Halsey S, Moiseyev G, Ma JX. Retinol-binding protein 4 induces inflammation in human endothelial cells by an NADPH oxidase- and nuclear factor kappa B-dependent and retinol-independent mechanism. *Mol Cell Biol* 2012; 32:5103-15. [PMID: 23071093].
15. Norseen J, Hosooka T, Hammarstedt A, Yore MM, Kant S, Aryal P, Kiernan UA, Phillips DA, Maruyama H, Kraus BJ, Usheva A, Davis RJ, Smith U, Kahn BB. Retinol-Binding Protein 4 Inhibits Insulin Signaling in Adipocytes by Inducing Proinflammatory Cytokines in Macrophages through a c-Jun N-Terminal Kinase- and Toll-Like Receptor 4-Dependent and Retinol-Independent Mechanism. *Mol Cell Biol* 2012; 32:2010-9. [PMID: 22431523].
16. Moraes-Vieira PM, Yore MM, Dwyer PM, Syed I, Aryal P, Kahn BB. RBP4 activates antigen-presenting cells, leading to adipose tissue inflammation and systemic insulin resistance. *Cell Metab* 2014; 19:512-26. [PMID: 24606904].
17. Chan CB, Liu X, Ensslin MA, Dillehay DL, Ormandy CJ, Sohn P, Serra R, Ye K. PIKE-A is required for prolactin-mediated STAT5a activation in mammary gland development. *EMBO J* 2010; 29:956-68. [PMID: 20075866].
18. Quadro L, Blaner WS, Hamberger L, Van Gelder RN, Vogel S, Piantadosi R, Gouras P, Colantuoni V, Gottesman ME. Muscle expression of human retinol-binding protein (RBP). Suppression of the visual defect of RBP knockout mice. *J Biol Chem* 2002; 277:30191-7. [PMID: 12048218].
19. Kawai T, Akira S. TLR signaling. *Semin Immunol* 2007; 19:24-32. [PMID: 17275323].
20. Akira S, Takeda K. Toll-like receptor signalling. *Nat Rev Immunol* 2004; 4:499-511. [PMID: 15229469].
21. Kawamoto T, Ii M, Kitazaki T, Iizawa Y, Kimura H. TAK-242 selectively suppresses Toll-like receptor 4-signaling mediated by the intracellular domain. *Eur J Pharmacol* 2008; 584:40-8. [PMID: 18299127].
22. Matsunaga N, Tsuchimori N, Matsumoto T, Ii M. TAK-242 (resatorvid), a small-molecule inhibitor of Toll-like receptor (TLR) 4 signaling, binds selectively to TLR4 and interferes with interactions between TLR4 and its adaptor molecules. *Mol Pharmacol* 2011; 79:34-41. [PMID: 20881006].
23. Peroval MY, Boyd AC, Young JR, Smith AL. A critical role for MAPK signalling pathways in the transcriptional regulation of toll like receptors. *PLoS One* 2013; 8:e51243-[PMID: 23405061].
24. Du M, Otolara L, Martin AA, Moiseyev G, Vanlandingham P, Wang Q, Farjo R, Yeganeh A, Quiambao A, Farjo KM. Transgenic Mice Overexpressing Serum Retinol-Binding Protein Develop Progressive Retinal Degeneration through a Retinoid-Independent Mechanism. *Mol Cell Biol* 2015; 35:2771-89. [PMID: 26055327].
25. Raz A, Shiratori T, Goodman DS. Studies on the protein-protein and protein-ligand interactions involved in retinol transport in plasma. *J Biol Chem* 1970; 245:1903-12. [PMID: 4985906].
26. Hyung SJ, Deroo S, Robinson CV. Retinol and retinol-binding protein stabilize transthyretin via formation of retinol transport complex. *ACS Chem Biol* 2010; 5:1137-46. [PMID: 20845945].
27. Berry DC, Croniger CM, Ghyselinck NB, Noy N. Transthyretin blocks retinol uptake and cell signaling by the holo-retinol-binding protein receptor STRA6. *Mol Cell Biol* 2012; 32:3851-9. [PMID: 22826435].

28. Myron Johnson A, Merlini G, Sheldon J, Ichihara K. Clinical indications for plasma protein assays: transthyretin (prealbumin) in inflammation and malnutrition. *Clin Chem Lab Med* 2007; 45:419-26. [PMID: 17378745].
29. Li ZZ, Lu XZ, Liu JB, Chen L. Serum Retinol-Binding Protein 4 Levels in Patients with Diabetic Retinopathy. *J Int Med Res* 2010; 38:95-9. [PMID: 20233518].
30. Schmidt AM, Vianna M, Gerlach M, Brett J, Ryan J, Kao J, Esposito C, Hegarty H, Hurlley W, Clauss M, Wang F, Pan YE, Tsang TC, Stern D. Isolation and characterization of two binding proteins for advanced glycosylation end products from bovine lung which are present on the endothelial cell surface. *J Biol Chem* 1992; 267:14987-97. [PMID: 1321822].
31. Xie J, Mendez JD, Mendez-Valenzuela V, Aguilar-Hernandez MM. Cellular signalling of the receptor for advanced glycation end products (RAGE). *Cell Signal* 2013; 25:2185-97. [PMID: 23838007].
32. Harja E, Bu DX, Hudson BI, Chang JS, Shen X, Hallam K, Kalea AZ, Lu Y, Rosario RH, Oruganti S, Nikolla Z, Belov D, Lalla E, Ramasamy R, Yan SF, Schmidt AM. Vascular and inflammatory stresses mediate atherosclerosis via RAGE and its ligands in apoE^{-/-} mice. *J Clin Invest* 2008; 118:183-94. [PMID: 18079965].
33. Yeh CH, Sturgis L, Haidacher J, Zhang XN, Sherwood SJ, Bjercke RJ, Juhasz O, Crow MT, Tilton RG, Denner L. Requirement for p38 and p44/p42 mitogen-activated protein kinases in RAGE-mediated nuclear factor-kappaB transcriptional activation and cytokine secretion. *Diabetes* 2001; 50:1495-504. [PMID: 11375353].
34. Ibrahim ZA, Armour CL, Phipps S, Sukkar MB. RAGE and TLRs: relatives, friends or neighbours? *Mol Immunol* 2013; 56:739-44. [PMID: 23954397].
35. Song PI, Abraham TA, Park Y, Zivony AS, Harten B, Edelhofer HF, Ward SL, Armstrong CA, Ansel JC. The expression of functional LPS receptor proteins CD14 and toll-like receptor 4 in human corneal cells. *Invest Ophthalmol Vis Sci* 2001; 42:2867-77. [PMID: 11687531].
36. Johnson AC, Heinzl FP, Diaconu E, Sun Y, Hise AG, Golenbock D, Lass JH, Pearlman E. Activation of toll-like receptor (TLR)2, TLR4, and TLR9 in the mammalian cornea induces MyD88-dependent corneal inflammation. *Invest Ophthalmol Vis Sci* 2005; 46:589-95. [PMID: 15671286].
37. Brito BE, Zamora DO, Bonnah RA, Pan Y, Planck SR, Rosenbaum JT. Toll-like receptor 4 and CD14 expression in human ciliary body and TLR-4 in human iris endothelial cells. *Exp Eye Res* 2004; 79:203-8. [PMID: 15325567].
38. Chang JH, McCluskey P, Wakefield D. Expression of toll-like receptor 4 and its associated lipopolysaccharide receptor complex by resident antigen-presenting cells in the human uvea. *Invest Ophthalmol Vis Sci* 2004; 45:1871-8. [PMID: 15161852].
39. Tu Z, Portillo JA, Howell S, Bu H, Subauste CS, Al-Ubaidi MR, Pearlman E, Lin F. Photoreceptor cells constitutively express functional TLR4. *J Neuroimmunol* 2011; 230:183-7. [PMID: 20801528].
40. Kumar A, Shamsuddin N. Retinal Muller glia initiate innate response to infectious stimuli via toll-like receptor signaling. *PLoS One* 2012; 7:e29830-[PMID: 22253793].
41. Lin S, Liang Y, Zhang J, Bian C, Zhou H, Guo Q, Xiong Y, Li S, Su B. Microglial TIR-domain-containing adapter-inducing interferon-beta (TRIF) deficiency promotes retinal ganglion cell survival and axon regeneration via nuclear factor-kappaB. *J Neuroinflammation* 2012; 9:39-[PMID: 22361049].
42. Ko MK, Saraswathy S, Parikh JG, Rao NA. The role of TLR4 activation in photoreceptor mitochondrial oxidative stress. *Invest Ophthalmol Vis Sci* 2011; 52:5824-35. [PMID: 21666244].
43. Kohno H, Chen Y, Kevany BM, Pearlman E, Miyagi M, Maeda T, Palczewski K, Maeda A. Photoreceptor proteins initiate microglial activation via Toll-like receptor 4 in retinal degeneration mediated by all-trans-retinal. *J Biol Chem* 2013; 288:15326-41. [PMID: 23572532].
44. Qi Y, Zhao M, Bai Y, Huang L, Yu W, Bian Z, Zhao M, Li X. Retinal ischemia/reperfusion injury is mediated by Toll-like receptor 4 activation of NLRP3 inflammasomes. *Invest Ophthalmol Vis Sci* 2014; 55:5466-75. [PMID: 25097240].
45. Ishizuka F, Shimazawa M, Inoue Y, Nakano Y, Ogishima H, Nakamura S, Tsuruma K, Tanaka H, Inagaki N, Hara H. Toll-like receptor 4 mediates retinal ischemia/reperfusion injury through nuclear factor-kappaB and spleen tyrosine kinase activation. *Invest Ophthalmol Vis Sci* 2013; 54:5807-16. [PMID: 23908181].
46. Stitt AW. The role of advanced glycation in the pathogenesis of diabetic retinopathy. *Exp Mol Pathol* 2003; 75:95-108. [PMID: 12834631].
47. Stitt AW. AGEs and diabetic retinopathy. *Invest Ophthalmol Vis Sci* 2010; 51:4867-74. [PMID: 20876889].
48. Zong H, Ward M, Stitt AW. AGEs, RAGE, and diabetic retinopathy. *Curr Diab Rep* 2011; 11:244-52. [PMID: 21590515].
49. Barber AJ. A new view of diabetic retinopathy: a neurodegenerative disease of the eye. *Prog Neuropsychopharmacol Biol Psychiatry* 2003; 27:283-90. [PMID: 12657367].
50. Barber AJ. Diabetic retinopathy: recent advances towards understanding neurodegeneration and vision loss. *Science China* 2015; 58:541-9. [PMID: 25951929].
51. Barber AJ, Antonetti DA, Kern TS, Reiter CE, Soans RS, Krady JK, Levison SW, Gardner TW, Bronson SK. The Ins2Akita mouse as a model of early retinal complications in diabetes. *Invest Ophthalmol Vis Sci* 2005; 46:2210-8. [PMID: 15914643].
52. Barber AJ, Lieth E, Khin SA, Antonetti DA, Buchanan AG, Gardner TW. Neural apoptosis in the retina during experimental and human diabetes. Early onset and effect of insulin. *J Clin Invest* 1998; 102:783-91. [PMID: 9710447].
53. Bearnse MA Jr, Adams AJ, Han Y, Schneck ME, Ng J, Bronson-Castain K, Barez S. A multifocal electroretinogram model predicting the development of diabetic retinopathy. *Prog Retin Eye Res* 2006; 25:425-48. [PMID: 16949855].

54. Bearnse MA Jr, Han Y, Schneck ME, Adams AJ. Retinal function in normal and diabetic eyes mapped with the slow flash multifocal electroretinogram. *Invest Ophthalmol Vis Sci* 2004; 45:296-304. [PMID: 14691187].
55. Bearnse MA Jr, Han Y, Schneck ME, Barez S, Jacobsen C, Adams AJ. Local multifocal oscillatory potential abnormalities in diabetes and early diabetic retinopathy. *Invest Ophthalmol Vis Sci* 2004; 45:3259-65. [PMID: 15326149].
56. Bresnick GH. Diabetic retinopathy viewed as a neurosensory disorder. *Arch Ophthalmol* 1986; 104:989-90. [PMID: 3729794].
57. Bresnick GH, Condit RS, Palta M, Korth K, Groo A, Syrjala S. Association of hue discrimination loss and diabetic retinopathy. *Arch Ophthalmol* 1985; 103:1317-24. [PMID: 4038123].
58. Bresnick GH, Korth K, Groo A, Palta M. Electroretinographic oscillatory potentials predict progression of diabetic retinopathy. Preliminary report. *Arch Ophthalmol* 1984; 102:1307-11. [PMID: 6383303].
59. Bresnick GH, Palta M. Predicting progression to severe proliferative diabetic retinopathy. *Arch Ophthalmol* 1987; 105:810-4. [PMID: 3579713].
60. Bresnick GH, Palta M. Temporal aspects of the electroretinogram in diabetic retinopathy. *Arch Ophthalmol* 1987; 105:660-4. [PMID: 3619742].
61. Di Leo MA, Falsini B, Caputo S, Ghirlanda G, Porciatti V, Greco AV. Spatial frequency-selective losses with pattern electroretinogram in type 1 (insulin-dependent) diabetic patients without retinopathy. *Diabetologia* 1990; 33:726-30. [PMID: 2073985].
62. Falsini B, Porciatti V, Scalia G, Caputo S, Minnella A, Di Leo MA, Ghirlanda G. Steady-state pattern electroretinogram in insulin-dependent diabetics with no or minimal retinopathy. *Doc Ophthalmol* 1989; 73:193-200. [PMID: 2638628].
63. Ghirlanda G, Di Leo MA, Caputo S, Cercone S, Greco AV. From functional to microvascular abnormalities in early diabetic retinopathy. *Diabetes Metab Rev* 1997; 13:15-35. [PMID: 9134346].
64. Greenstein VC, Shapiro A, Zaidi Q, Hood DC. Psychophysical evidence for post-receptor sensitivity loss in diabetics. *Invest Ophthalmol Vis Sci* 1992; 33:2781-90. [PMID: 1526727].
65. Han Y, Adams AJ, Bearnse MA Jr, Schneck ME. Multifocal electroretinogram and short-wavelength automated perimetry measures in diabetic eyes with little or no retinopathy. *Arch Ophthalmol* 2004; 122:1809-15. [PMID: 15596584].
66. Han Y, Bearnse MA Jr, Schneck ME, Barez S, Jacobsen CH, Adams AJ. Multifocal electroretinogram delays predict sites of subsequent diabetic retinopathy. *Invest Ophthalmol Vis Sci* 2004; 45:948-54. [PMID: 14985316].
67. Han Y, Schneck ME, Bearnse MA Jr, Barez S, Jacobsen CH, Jewell NP, Adams AJ. Formulation and evaluation of a predictive model to identify the sites of future diabetic retinopathy. *Invest Ophthalmol Vis Sci* 2004; 45:4106-12. [PMID: 15505062].
68. Hombrebueno JR, Chen M, Penalva RG, Xu H. Loss of synaptic connectivity, particularly in second order neurons is a key feature of diabetic retinal neuropathy in the Ins2Akita mouse. *PLoS One* 2014; 9:e97970-[PMID: 24848689].
69. Lieth E, LaNoue KF, Antonetti DA, Ratz M. Diabetes reduces glutamate oxidation and glutamine synthesis in the retina. The Penn State Retina Research Group. *Exp Eye Res* 2000; 70:723-30. [PMID: 10843776].
70. Mizutani M, Gerhardinger C, Lorenzi M. Muller cell changes in human diabetic retinopathy. *Diabetes* 1998; 47:445-9. [PMID: 9519752].
71. Rungger-Brandle E, Dosso AA, Leuenberger PM. Glial reactivity, an early feature of diabetic retinopathy. *Invest Ophthalmol Vis Sci* 2000; 41:1971-80. [PMID: 10845624].
72. VanGuilder HD, Brucklacher RM, Patel K, Ellis RW, Freeman WM, Barber AJ. Diabetes downregulates presynaptic proteins and reduces basal synapsin I phosphorylation in rat retina. *Eur J Neurosci* 2008; 28:1-11. [PMID: 18662330].
73. Zeng HY, Green WR, Tso MO. Microglial activation in human diabetic retinopathy. *Arch Ophthalmol* 2008; 126:227-32. [PMID: 18268214].
74. Zeng XX, Ng YK, Ling EA. Neuronal and microglial response in the retina of streptozotocin-induced diabetic rats. *Vis Neurosci* 2000; 17:463-71. [PMID: 10910112].
75. Stuck BJ, Kahn BB. Retinol-binding protein 4 (RBP4): a biomarker for subclinical atherosclerosis? *Am J Hypertens* 2009; 22:948-9. [PMID: 19701163].
76. Bogdanov P, Corraliza L, Villena JA, Carvalho AR, Garcia-Arumi J, Ramos D, Ruberte J, Simo R, Hernandez C. The db/db mouse: a useful model for the study of diabetic retinal neurodegeneration. *PLoS One* 2014; 9:e97302-[PMID: 24837086].
77. Bogdanov P, Hernandez C, Corraliza L, Carvalho AR, Simo R. Effect of fenofibrate on retinal neurodegeneration in an experimental model of type 2 diabetes. *Acta Diabetol* 2015; 52:113-22. [PMID: 25029994].
78. Cheung AK, Fung MK, Lo AC, Lam TT, So KF, Chung SS, Chung SK. Aldose reductase deficiency prevents diabetes-induced blood-retinal barrier breakdown, apoptosis, and glial reactivation in the retina of db/db mice. *Diabetes* 2005; 54:3119-25. [PMID: 16249434].
79. Clements RS Jr, Robison WG Jr, Cohen MP. Anti-glycated albumin therapy ameliorates early retinal microvascular pathology in db/db mice. *J Diabetes Complications* 1998; 12:28-33. [PMID: 9442812].
80. Midena E, Segato T, Radin S, di Giorgio G, Meneghini F, Piermarocchi S, Belloni AS. Studies on the retina of the diabetic db/db mouse. I. Endothelial cell-pericyte ratio. *Ophthalmic Res* 1989; 21:106-11. [PMID: 2734001].
81. Yang Q, Xu Y, Xie P, Cheng H, Song Q, Su T, Yuan S, Liu Q. Retinal Neurodegeneration in db/db Mice at the Early Period of Diabetes. *J Ophthalmol* 2015; 2015:757412-[PMID: 25821591].

82. Feit-Leichman RA, Kinouchi R, Takeda M, Fan Z, Mohr S, Kern TS, Chen DF. Vascular damage in a mouse model of diabetic retinopathy: relation to neuronal and glial changes. *Invest Ophthalmol Vis Sci* 2005; 46:4281-7. [PMID: 16249509].
83. Jousseaume AM, Poulaki V, Le ML, Koizumi K, Esser C, Janicki H, Schraermeyer U, Kociok N, Fauser S, Kirchhof B, Kern TS, Adamis AP. A central role for inflammation in the pathogenesis of diabetic retinopathy. *FASEB J* 2004; 18:1450-2. [PMID: 15231732].
84. Lai AK, Lo AC. Animal models of diabetic retinopathy: summary and comparison. *J Diabetes Res* 2013; 2013:106594-[PMID: 24286086].
85. Li Q, Verma A, Han PY, Nakagawa T, Johnson RJ, Grant MB, Campbell-Thompson M, Jarajapu YP, Lei B, Hauswirth WW. Diabetic eNOS-knockout mice develop accelerated retinopathy. *Invest Ophthalmol Vis Sci* 2010; 51:5240-6. [PMID: 20435587].
86. Tang J, Allen Lee C, Du Y, Sun Y, Pearlman E, Sheibani N, Kern TS. MyD88-dependent pathways in leukocytes affect the retina in diabetes. *PLoS One* 2013; 8:e68871-[PMID: 23874797].

Articles are provided courtesy of Emory University and the Zhongshan Ophthalmic Center, Sun Yat-sen University, P.R. China. The print version of this article was created on 31 March 2017. This reflects all typographical corrections and errata to the article through that date. Details of any changes may be found in the online version of the article.